# Title: Animal septins contain functional transmembrane domains

**Authors:** Jenna A. Perry[1]*, Michael E. Werner[1], Shizue Omi[2], Bryan W. Heck[1], Paul S. Maddox[1], Manos Mavrakis[2], Amy S. Maddox[1]*

**Affiliations:**

[1]Department of Biology, The University of North Carolina at Chapel Hill; Chapel Hill, North Carolina, 27599 USA

[2]Institut Fresnel, CNRS UMR7249, Aix Marseille Univ, Centrale Med, 13013 Marseille, France

*Corresponding author. Email: jenna_perry@unc.edu, asm@unc.edu

**Abstract:** Septins, a conserved family of filament-forming proteins, contribute to eukaryotic cell division, polarity, and membrane trafficking. Septins scaffold other proteins to cellular membranes, but it is unknown how septins associate with membranes. We identified and characterized an isoform of *Caenorhabditis elegans* septin UNC-61 that was predicted to contain a transmembrane domain (TMD). The TMD isoform is expressed in a subset of tissues where the known septins were known to act, and TMD function was required for tissue integrity of the egg-laying apparatus. We found TMD-containing septins across opisthokont phylogeny and demonstrated that the TMD-containing sequence of a primate TMD-septin is sufficient for localization to cellular membranes. Together, our findings reveal a novel mechanism of septin-membrane association with profound implications for septin dynamics and regulation.

**Main Text:** Cells comprise exceptionally complex mixtures of proteins, lipids, sugars, and small molecules that must combine to create multicomponent machines and to execute multistep signaling and synthesis cascades. The efficiency of such cellular tasks is often boosted by scaffolding via polymeric systems including the cytoskeleton. Septins are a highly conserved family of proteins that form palindromic hetero-oligomeric rods, which anneal into non-polar filaments and gauzes. Via their association with the plasma membrane, septin filaments recognize micron-scale membrane curvature, create diffusion barriers, and regulate cell morphogenic events via scaffolding other cytoskeletal polymers (i.e. F-actin and microtubules) and biochemical regulators of cell division, cell migration, and polarity establishment (*1*, *2*). While interaction with cellular membranes is thought to be crucial for septin polymer dynamics and function, how septins associate with membranes is not understood. Three polybasic regions (PB1, PB2, PB3) and an amphipathic helix (AH), are each sufficient for membrane interaction *in vitro*, and while the AH domain has been implicated in conferring membrane curvature sensing *in vivo* in the filamentous fungus *Ashbya*, the importance of all of these domains in the context of intact septin complexes *in vivo* is still lacking (*3–9*). We explored how septins associate with membranes and discovered that some septins have functional transmembrane domains (TMDs).

### *C. elegans* UNC-61a contains a TMD that drives membrane localization

To study the mechanisms of septin-membrane association, we interrogated the uniquely simple set of septin genes of the nematode *Caenorhabditis elegans.* While other animal and fungal model organisms have five or more septin genes, often with many splice isoforms, the *C. elegans* genome contains only two septin genes, *unc-59* and *unc-61*. UNC-59 and UNC-61 proteins are interdependent *in vivo* and form palindromic tetramers *in vitro* with two UNC-61 proteins in the center and UNC-59 on each end (*10*, *11*). *C. elegans* septins exhibit behaviors shared by other organisms' septins, including enrichment in and requirement for normal function of the cytokinetic ring (*10–13*). We examined the *C. elegans* septin gene loci and found that *unc-61* encodes three isoforms: a, b, and c (Figure S1). *unc-61a* is transcribed from an alternative start site upstream of the start codon of isoforms *unc-61b* and *unc-61c*, which differ only by a single stretch of four amino acids, a distinction that we do not interrogate here. Hereafter, we refer to UNC-61b and UNC-61c collectively as UNC-61b/c. AlphaFold and a deep learning model for transmembrane topology prediction and classification (DeepTMHMM (*14*)), predicted that the N-terminal amino acids of UNC-61a encode an α-helix that is expected with 99-100% certainty to form a transmembrane domain (TMD; Figure 1A and B). Alignment of homologous septin sequences from several related nematode species revealed that this putative TMD sequence is well conserved in this genus (Figure 1C). While the presence of a putative TMD has been predicted for at least 30 non-opisthokont (e.g. Chromista and Archaeplastida) septins (*15–17*), their relevance has not been tested experimentally. Importantly, to date, no TMD-containing septin (TMD-septin, hereafter) has been identified within opisthokont (animal and fungal) lineages and functional implications of such a septin have not been investigated.

To test the functionality of the putative TMD of *unc-61a*, we assessed whether this sequence was sufficient to drive membrane association. We created a transgene encoding residues

1-48 of UNC-61a (the first exon of *unc-61a*) and HaloTag (Figure 1D). We co-labeled the transfected cells with phalloidin to visualize F-actin, DAPI for DNA, and anti-GM130, a cis-Golgi marker, to examine UNC-61a$_{1-48}$::HaloTag localization (Figure 1D). HaloTag alone primarily localized diffusely to the cytoplasm, while UNC-61a$_{1-48}$::HaloTag localized around the nucleus and proximal to the GM130 signal (Figure 1D). To further test if the UNC-61a$_{1-48}$::HaloTag directly interacted with cellular membranes, we separated cells into cytoplasmic and membranous fractions (Figure 1E). In contrast to γ-tubulin, which is enriched in the cytoplasmic fraction, UNC-61a$_{1-48}$::HaloTag was enriched in the membrane fraction and was undetectable in the cytoplasmic fraction, as was the Golgi matrix protein GM130. These findings demonstrate that the predicted TMD of *C. elegans* UNC-61a can confer localization to membranes.

**UNC-61a TMD is responsible for UNC-61a function in vulval morphology maintenance**

To test whether a septin bearing a TMD is functionally important, we first examined how the localization of UNC-61a compared to that of UNC-61b/c and UNC-59. To minimize interference with the N-terminal TMD, we generated animals expressing UNC-61a intramolecularly tagged with a *C. elegans* codon optimized GFP and placed under the control of the *unc-61a* promoter at a Mos1-mediated single copy insertion (MosSCI) site on chromosome II (Figure S2). A similar MosSCI approach was utilized to create an exogenous copy of UNC-61b/c tagged at its N-terminus with the monomeric and *C. elegans* codon optimized wrmScarlet under control of the *unc-61b/c* promoter at a MosSCI site also on chromosome II (wrmScarlet::*unc-61b/c;* Figure S2). UNC-61a::GFP was highly enriched in the terminal bulb of the pharynx, often decorating linear structures, and in the vulva in adult hermaphrodite *C. elegans*, while wrmScarlet::UNC-61b/c was less enriched in those structures (Figure 2A). Conversely, wrmScarlet::UNC-61b/c decorated the *C. elegans* oogenic germline; UNC-61a::GFP was undetectable there (Figure 2A; (*11*, *18*)). Interestingly, fluorescently-tagged UNC-59 (UNC-59::GFP) expressed from its endogenous locus localizes to tissues where either UNC-61a or UNC-61b/c is individually enriched: UNC-59::GFP is present in pharynx, germline, and vulva (Figure 2A). The differential localization patterns of the UNC-61 isoforms suggest that they have distinct physiological roles in the tissues where they are expressed and that UNC-59 functions with both UNC-61a and UNC-61b/c, in different tissues.

We next tested whether the loss of the TMD from UNC-61a affected its function in *C. elegans*. Depletion or mutation of either *unc-59* or *unc-61* results in uncoordinated movement, reduced fertility, and gross morphological defects of the egg-laying apparatus (uterus and vulva) (*11*, *18–22*). UNC-61 depletion and mutations used to date have altered or removed expression and function of all three isoforms (*11*, *23–25*). We used CRISPR/Cas9 genome editing to excise amino acid residues 1-524 (numbering with respect to *unc-61a* translation) to create *unc-61* null animals, introduced a stop codon at amino acid residue 2 to create *unc-61a* null animals (UNC-61aΔ; Figure S3), and excised the bases encoding amino acids 7-29 to create a genotype specifically lacking the TMD of UNC-61a (UNC-61a ΔTMD; Figure S3). *unc-61* null (61Δ) animals exhibited the range and severity of phenotypes, including the retention of embryos in the uterus (egl) and larvae present inside the uterus (bag) (Figure 2B), that were previously reported

for random mutagenesis-generated hypomorphic alleles (*11*, *18*, *19*, *22*, *23*, *26*). While *unc-61a* null (UNC-61a Δ) or UNC-61a ΔTMD animals had normal fertility and animal motility (Figure S4), they exhibited abnormally protruded vulvas (pvl; Figure 2B). Thus, the array of phenotypes exhibited by animals lacking all UNC-61 isoforms is partially due to absence of UNC-61b/c (fertility and motility defects) and partially due to the absence of UNC-61a (vulval morphology), whose function depends on its TMD, as excision of the TMD phenocopies the *unc-61a* null allele.

To understand the basis for the pvl phenotype in UNC-61a ΔTMD animals, we examined vulval morphology. High resolution imaging of adult animals expressing Lifeact::GFP to label F-actin in epidermal cells revealed that the vulva of the UNC-61a ΔTMD animals rested in an abnormal, open conformation. In addition, the surrounding tissue frequently appeared detached from the ventral cuticle (Figure 2C). Together with our observation that UNC-61a specifically localizes to the vulval lumen (Figure 2A), these results suggest that UNC-61a contributes to vulval morphology. In sum, our work demonstrates the functional importance of a TMD-septin.

**Septins throughout phylogeny are predicted to contain transmembrane domains (TMD)**

Given the conservation of sequence and function of septins, we reasoned that TMD-septins could be present throughout opisthokont phylogeny. We surveyed over 34,000 sequences containing a "septin-type guanine nucleotide-binding (G) domain" on UniProt for the presence of TMDs (*27*). Putative TMDs were present in septin genes from many organisms across phylogeny (Figure 3A). Of the 2320 eukaryotic species predicted to express septin-like proteins, 447, or nearly 20%, were predicted to possess at least one TMD-septin. TMD-septins were not predicted in many well-established model organisms including budding yeast, fruit fly, and mouse, but predicted in some, including the fission yeast *Schizosacchromyces japonicus* and the small primate *Carlito syrichta*, a non-model-animal tarsier (Figure 3A and B).

To test whether the predicted TMD of a primate septin is sufficient for localization to membranes, we examined *Carlito syrichta* SEPT10 (*Cs*SEPT10) whose C-terminus contains a TMD sequence(Figure S5 ). We created a fusion protein wherein a fluorescent protein was added to the TMD-containing C-terminus of the *Cs*SEPT10 and expressed GFP-*Cs*SEPT10$_C$ in U2OS cells (Figure 3C). The predicted TMD was sufficient to localize the fluorescent protein to endomembranes, particularly the endoplasmic reticulum and mitochondria (Figure 3C). We next tested whether the TMD of *Cs*SEPT10 could drive membrane localization of a septin lacking a TMD. Despite the close phylogenetic relationship between humans and *C. syrichta*, *Hs*SEPT10 is not predicted to contain a C-terminal TMD (Figure 3D and E, Figure S5). Accordingly, *Hs*SEPT10 localizes to actomyosin stress fibers (Figure 3E (*28*, *29*)). We created a fluorescently labeled chimeric SEPT10 by adding the *C. syrichta* C-terminal TMD to *Hs*SEPT10 (Figure 3E). The *C. syrichta* SEPT10 TMD was sufficient to re-localize *Hs*SEPT10 entirely from stress fibers to endomembranes (Figure 3E). Together, these results demonstrate that primates possess a TMD-septin. Furthermore, the presence of the TMD in septin genes throughout phylogeny suggests that the ancestral septin had a transmembrane domain that has been lost in some lineages and over the course of gene duplications.

## Discussion

The presence of a validated TMD sufficient for membrane interaction in a multicellular organism prompts reconsideration of mechanisms and regulation by which septins interact with cellular membranes. Membrane association via a TMD is predicted to have dramatically different dynamics, requiring membrane retrieval or protein cleavage to turn over. As a result, the potentially constitutive membrane association of TMD-septins prompts speculation of novel roles. For example, the localization of *C. elegans* UNC-61a to the terminal bulb of the pharynx and the apical membrane of the vulval epithelial cells suggests a role in these highly dynamic tissues' extracellular matrix secretion (*30–34*). The two motifs (an amphipathic helix (AH) and polybasic regions) previously implicated in mediating septin-membrane interactions had unclear functional relevance *in vivo*. In cells lacking a TMD-septin, residual membrane association may be conferred by septins' indirect association with membranes via binding to cytoskeletal partners including the crosslinking protein anillin that directly binds the plasma membrane. Across phylogeny, most species were predicted to express only one TMD-septin among their large collection of septin genes and splice isoforms. Thus, TMD-septins may be present at low stoichiometry relative to non-TMD septins with which they can co-polymerize. Even at low stoichiometry, TMD-septins could confer and stabilize membrane association of septin polymers in a manner analogous to how tubulin isotypes with low expression can alter microtubule polymer dynamics with profound cellular and tissue-level implications such as in cancer prognosis (*31*, *35–38*).

## References and Notes


1. B. L. Woods, A. S. Gladfelter, The state of the septin cytoskeleton from assembly to function. *Current Opinion in Cell Biology* **68**, 105–112 (2021).
2. B. Benoit, C. Poüs, A. Baillet, Septins as membrane influencers: direct play or in association with other cytoskeleton partners. *Frontiers in Cell and Developmental Biology* **11** (2023).
3. Y. Tanaka-Takiguchi, M. Kinoshita, K. Takiguchi, Septin-Mediated Uniform Bracing of Phospholipid Membranes. *Current Biology* **19**, 140–145 (2009).
4. A. Casamayor, M. Snyder, Molecular Dissection of a Yeast Septin: Distinct Domains Are Required for Septin Interaction, Localization, and Function. *Mol Cell Biol* **23**, 2762–2777 (2003).
5. A. Akil, J. Peng, M. Omrane, C. Gondeau, C. Desterke, M. Marin, H. Tronchère, C. Taveneau, S. Sar, P. Briolotti, S. Benjelloun, A. Benjouad, P. Maurel, V. Thiers, S. Bressanelli, D. Samuel, C. Bréchot, A. Gassama-Diagne, Septin 9 induces lipid droplets growth by a phosphatidylinositol-5-phosphate and microtubule-dependent mechanism hijacked by HCV. *Nat Commun* **7**, 12203 (2016).
6. J. Zhang, C. Kong, H. Xie, P. S. McPherson, S. Grinstein, W. S. Trimble, Phosphatidylinositol polyphosphate binding to the mammalian septin H5 is modulated by GTP. *Current Biology* **9**, 1458–1467 (1999).
7. K. S. Cannon, B. L. Woods, J. M. Crutchley, A. S. Gladfelter, An amphipathic helix enables septins to sense micrometer-scale membrane curvature. *Journal of Cell Biology* **218**, 1128–1137 (2019).
8. B. L. Woods, K. S. Cannon, E. J. D. Vogt, J. M. Crutchley, A. S. Gladfelter, Interplay of septin amphipathic helices in sensing membrane-curvature and filament bundling. *MBoC* **32**, br5 (2021).
9. I. A. Cavini, M. G. Fontes, A. E. Zeraik, J. L. S. Lopes, A. P. U. Araujo, Novel lipid-interaction motifs within the C-terminal domain of Septin10 from *Schistosoma mansoni*. *Biochimica et Biophysica Acta (BBA) - Biomembranes* **1866**, 184371 (2024).
10. C. M. John, R. K. Hite, C. S. Weirich, D. J. Fitzgerald, H. Jawhari, M. Faty, D. Schläpfer, R. Kroschewski, F. K. Winkler, T. Walz, Y. Barral, M. O. Steinmetz, The Caenorhabditis elegans septin complex is nonpolar. *EMBO J* **26**, 3296–3307 (2007).
11. T. Q. Nguyen, H. Sawa, H. Okano, J. G. White, The C. elegans septin genes, unc-59 and unc-61, are required for normal postembryonic cytokineses and morphogenesis but have no essential function in embryogenesis. *Journal of Cell Science* **113**, 3825–3837 (2000).

12. S. N. Jordan, T. Davies, Y. Zhuravlev, J. Dumont, M. Shirasu-Hiza, J. C. Canman, Cortical PAR polarity proteins promote robust cytokinesis during asymmetric cell division. *Journal of Cell Biology* **212**, 39–49 (2016).
13. L. Lewellyn, A. Carvalho, A. Desai, A. S. Maddox, K. Oegema, The chromosomal passenger complex and centralspindlin independently contribute to contractile ring assembly. *Journal of Cell Biology* **193**, 155–169 (2011).
14. J. Hallgren, K. D. Tsirigos, M. D. Pedersen, J. J. A. Armenteros, P. Marcatili, H. Nielsen, A. Krogh, O. Winther, DeepTMHMM predicts alpha and beta transmembrane proteins using deep neural networks. bioRxiv [Preprint] (2022). https://doi.org/10.1101/2022.04.08.487609.
15. R. Nishihama, M. Onishi, J. R. Pringle, New Insights into the Phylogenetic Distribution and Evolutionary Origins of the Septins. *Biol Chem* **392**, 681–687 (2011).
16. S. Delic, B. Shuman, S. Lee, S. Bahmanyar, M. Momany, M. Onishi, The Evolutionary Origins and Ancestral Features of Septins. bioRxiv [Preprint] (2024). https://doi.org/10.1101/2024.03.25.586683.
17. D. Włoga, I. Strzyżewska-Jówko, J. Gaertig, M. Jerka-Dziadosz, Septins Stabilize Mitochondria in Tetrahymena thermophila. *Eukaryotic Cell* **7**, 1373–1386 (2008).
18. F. P. Finger, K. R. Kopish, J. G. White, A role for septins in cellular and axonal migration in C. elegans. *Developmental Biology* **261**, 220–234 (2003).
19. S. Brenner, The genetics of Caenorhabditis elegans. *Genetics* **77**, 71–94 (1974).
20. J. E. Sulston, H. R. Horvitz, Abnormal cell lineages in mutants of the nematode Caenorhabditis elegans. *Developmental Biology* **82**, 41–55 (1981).
21. J. G. White, H. R. Horvitz, J. E. Sulston, Neurone differentiation in cell lineage mutants of Caenorhabditis elegans. *Nature* **297**, 584–587 (1982).
22. J. A. Perry, M. E. Werner, L. Rivenbark, A. S. Maddox, Caenorhabditis elegans septins contribute to the development and structure of the oogenic germline. *Cytoskeleton* **80**, 215–227 (2023).
23. A. Zaatri, J. A. Perry, A. S. Maddox, Septins and a formin have distinct functions in anaphase chiral cortical rotation in the *Caenorhabditis elegans* zygote. *MBoC* **32**, 1283–1292 (2021).
24. A. G. Fraser, R. S. Kamath, P. Zipperlen, M. Martinez-Campos, M. Sohrmann, J. Ahringer, Functional genomic analysis of C. elegans chromosome I by systematic RNA interference. *Nature* **408**, 325–330 (2000).
25. R. S. Kamath, A. G. Fraser, Y. Dong, G. Poulin, R. Durbin, M. Gotta, A. Kanapin, N. Le Bot, S. Moreno, M. Sohrmann, D. P. Welchman, P. Zipperlen, J. Ahringer, Systematic functional analysis of the Caenorhabditis elegans genome using RNAi. *Nature* **421**, 231–237 (2003).
26. A. S. Maddox, L. Lewellyn, A. Desai, K. Oegema, Anillin and the Septins Promote Asymmetric Ingression of the Cytokinetic Furrow. *Developmental Cell* **12**, 827–835 (2007).
27. The UniProt Consortium, UniProt: the Universal Protein Knowledgebase in 2023. *Nucleic Acids Research* **51**, D523–D531 (2023).
28. E. Sjöstedt, W. Zhong, L. Fagerberg, M. Karlsson, N. Mitsios, C. Adori, P. Oksvold, F. Edfors, A. Limiszewska, F. Hikmet, J. Huang, Y. Du, L. Lin, Z. Dong, L. Yang, X. Liu, H. Jiang, X. Xu, J. Wang, H. Yang, L. Bolund, A. Mardinoglu, C. Zhang, K. von Feilitzen, C. Lindskog, F. Pontén, Y. Luo, T. Hökfelt, M. Uhlén, J. Mulder, An atlas of the protein-coding genes in the human, pig, and mouse brain. *Science* **367**, eaay5947 (2020).
29. SEPTIN10 protein expression summary - The Human Protein Atlas. https://www.proteinatlas.org/ENSG00000186522-SEPTIN10.
30. J. D. Cohen, A. P. Sparacio, A. C. Belfi, R. Forman-Rubinsky, D. H. Hall, H. Maul-Newby, A. R. Frand, M. V. Sundaram, A multi-layered and dynamic apical extracellular matrix shapes the vulva lumen in Caenorhabditis elegans. *eLife* **9**, e57874 (2020).
31. A. P. Sparacio, N. F. Trojanowski, K. Snetselaar, M. D. Nelson, D. M. Raizen, Teething during sleep: Ultrastructural analysis of pharyngeal muscle and cuticular grinder during the molt in Caenorhabditis elegans. *PLoS ONE* **15**, e0233059 (2020).
32. E. Tokhtaeva, J. Capri, E. A. Marcus, J. P. Whitelegge, V. Khuzakhmetova, E. Bukharaeva, N. Deiss-Yehiely, L. A. Dada, G. Sachs, E. Fernandez-Salas, O. Vagin, Septin Dynamics Are Essential for Exocytosis. *Journal of Biological Chemistry* **290**, 5280–5297 (2015).
33. N. D. Amin, Y.-L. Zheng, S. Kesavapany, J. Kanungo, T. Guszczynski, R. K. Sihag, P. Rudrabhatla, W. Albers, P. Grant, H. C. Pant, Cyclin-Dependent Kinase 5 Phosphorylation of Human Septin SEPT5 (hCDCrel-1) Modulates Exocytosis. *J. Neurosci.* **28**, 3631–3643 (2008).
34. C. L. Beites, H. Xie, R. Bowser, W. S. Trimble, The septin CDCrel-1 binds syntaxin and inhibits exocytosis. *Nat Neurosci* **2**, 434–439 (1999).
35. A. Latremoliere, L. Cheng, M. DeLisle, C. Wu, S. Chew, E. B. Hutchinson, A. Sheridan, C. Alexandre, F. Latremoliere, S.-H. Sheu, S. Golidy, T. Omura, E. A. Huebner, Y. Fan, M. C. Whitman, E. Nguyen, C. Hermawan, C. Pierpaoli, M. A. Tischfield, C. J. Woolf, E. C. Engle, Neuronal-Specific TUBB3 Is Not Required for Normal Neuronal Function but Is Essential for Timely Axon Regeneration. *Cell Reports* **24**, 1865-1879.e9 (2018).

36. L. J. Leandro-García, S. Leskelä, I. Landa, C. Montero-Conde, E. López-Jiménez, R. Letón, A. Cascón, M. Robledo, C. Rodríguez-Antona, Tumoral and tissue-specific expression of the major human β-tubulin isotypes. *Cytoskeleton* **67**, 214–223 (2010).
37. A. Vemu, J. Atherton, J. O. Spector, C. A. Moores, A. Roll-Mecak, Tubulin isoform composition tunes microtubule dynamics. *MBoC* **28**, 3564–3572 (2017).
38. S.-C. Ti, G. M. Alushin, T. M. Kapoor, Human β-Tubulin Isotypes Can Regulate Microtubule Protofilament Number and Stability. *Developmental Cell* **47**, 175-190.e5 (2018).
39. L. Käll, A. Krogh, E. L. L. Sonnhammer, A Combined Transmembrane Topology and Signal Peptide Prediction Method. *Journal of Molecular Biology* **338**, 1027–1036 (2004).
40. A. Krogh, B. Larsson, G. von Heijne, E. L. L. Sonnhammer, Predicting transmembrane protein topology with a hidden markov model: application to complete genomes11Edited by F. Cohen. *Journal of Molecular Biology* **305**, 567–580 (2001).
41. I. Letunic, P. Bork, Interactive Tree Of Life (iTOL) v5: an online tool for phylogenetic tree display and annotation. *Nucleic Acids Research* **49**, W293–W296 (2021).
42. D. M. Emms, S. Kelly, SHOOT: phylogenetic gene search and ortholog inference. *Genome Biology* **23**, 85 (2022).
43. R. C. Edgar, MUSCLE: multiple sequence alignment with high accuracy and high throughput. *Nucleic Acids Research* **32**, 1792–1797 (2004).
44. K. Tamura, G. Stecher, S. Kumar, MEGA11: Molecular Evolutionary Genetics Analysis Version 11. *Molecular Biology and Evolution* **38**, 3022–3027 (2021).
45. G. A. Dokshin, K. S. Ghanta, K. M. Piscopo, C. C. Mello, Robust Genome Editing with Short Single-Stranded and Long, Partially Single-Stranded DNA Donors in Caenorhabditis elegans. *Genetics* **210**, 781–787 (2018).
46. Benchling. https://benchling.com.
47. B. Madhu, M. F. Lakdawala, T. L. Gumienny, Small-Scale Extraction of Caenorhabditis elegans Genomic DNA. *JoVE*, 63716 (2022).

**Acknowledgments:** The authors would like to thank the following individuals for fruitful discussions on this work: Lil Fritz-Laylin, Amy Gladfelter and her lab, Bob Goldstein, Kacy Gordon, Michelle Momany, Brent Shuman, Masa Onishi, and Samed Delic. We would also like to thank members of the Maddox labs for fruitful discussion, particularly Linnea Wethekam for critical reading of this manuscript. Some strains used in this work were provided by the Caenorhabditis Genetics Center (CGC), which is funded by NIH Office of Research Infrastructure Programs (P40 OD010440)

**Funding:**

National Institutes of Health grant 1R35GM144238-01 (ASM)

UNC Lineberger Comprehensive Cancer Center Discovery Award (ASM)

National Science Foundation grant 2153790 (ASM)

National Institutes of Health grant 1F32GM143910 (JAP)

French National Research Agency (ANR) grant ANR-22-CE13-0039 (MM)

**Author contributions:**

Conceptualization: JAP

Methodology: JAP, MEW

Investigation: JAP, MEW, SO, BWH, MM

Visualization: JAP

Funding acquisition: JAP, ASM

Supervision: PSM, MM, ASM

Resources: PSM, MM, ASM

Writing – original draft: JAP

Writing – review & editing: JAP, MEW, MM, ASM

**Competing interests:** The authors have declared no competing interests.

**Data and materials availability:** All data are available in the main text or the supplementary materials. Information and reagent requests should be directed to the corresponding author(s).

**Supplementary Materials**

Materials and Methods

Figs. S1 to S5

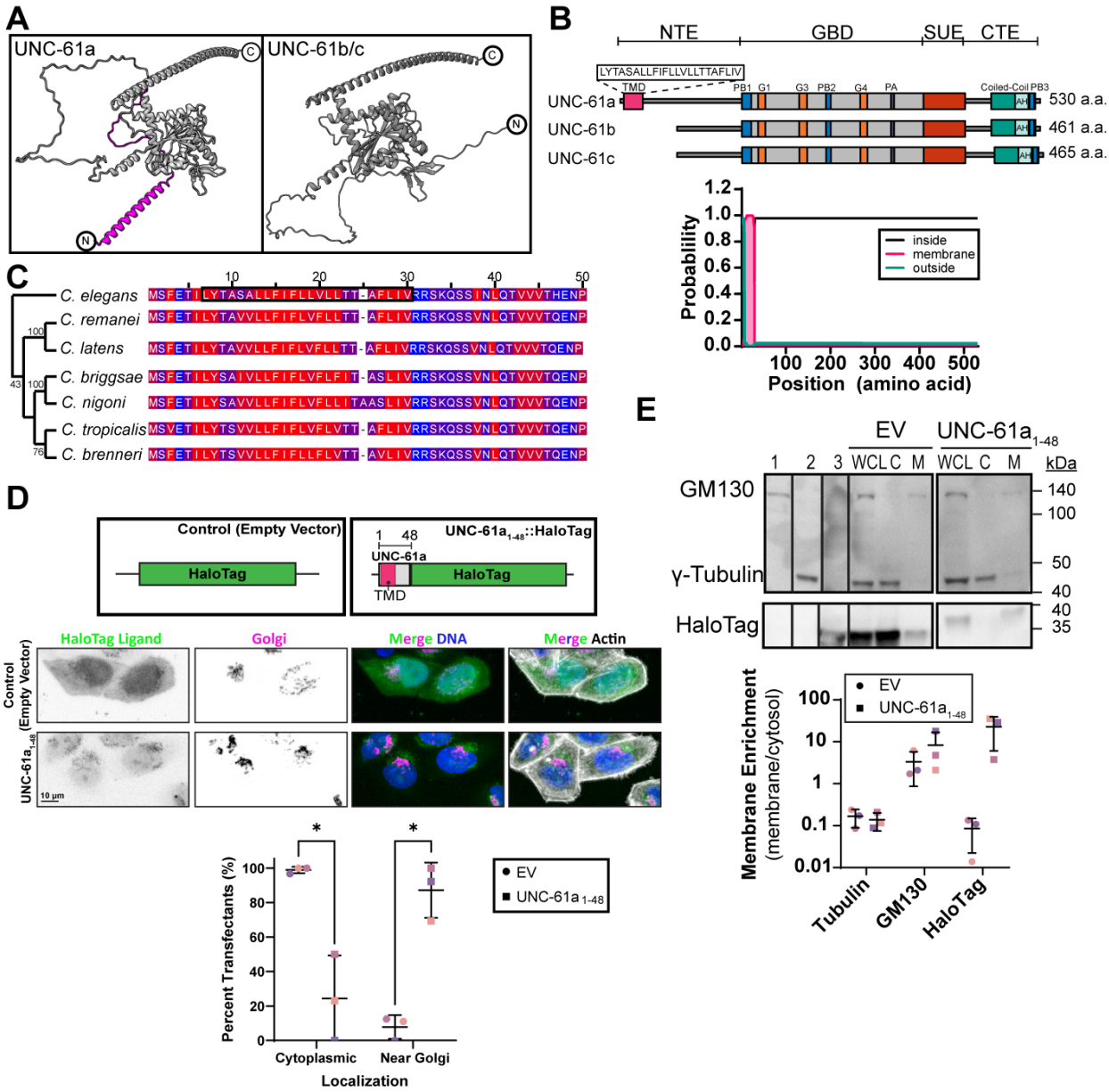


**Fig. 1. *C. elegans* UNC-61a contains a transmembrane domain. (A)** AlphaFold structures of UNC-61a and UNC-61b/c. Magenta: N-terminal alpha-helix of UNC-61a. **(B)** (top) Illustration of UNC-61a. Motifs are colored as follows: pink: transmembrane domain (TMD), grey: GTP-binding domain, red: SUE, blue: PB1/2/3, orange: GTPase domains, purple: polyacidic region [PA], teal: coiled-coil domain, light green: amphipathic helix (AH)). Brackets at top of schematic denote septin domains (NTE: N-terminal extension, GBD: GTP-binding domain, SUE: septin unique element, CTE: C-terminal extension) (bottom) DeepTMHMM output probability of TMD for *C. elegans* UNC-61. Teal: extracellular, pink: TMD, black: cytosolic. **(C)** (right) Alignment of UNC-61 homologs in *C. elegans* and closely related nematodes, first 50 amino acids (black: TMD, red: hydrophobic, blue: hydrophilic). (left) Neighbor-joining tree of evolutionary relationships. **(D)** (top) Illustration of control and UNC-61a $_{1\text{-}48}$::HaloTag constructs, where transient expression constructs highlighting the position of HaloTag (green), TMD (magenta), and UNC-61a fragment

(grey). (middle) HeLa cells transiently expressing HaloTag or UNC-61a $TMD_{1-48}$:HaloTag (green: HaloTag ligand; magenta: anti-GM130, white: phalloidin, blue: DAPI. Images are maximum intensity projections, inverted contrast, and scaled to display minimum and maximum pixel intensities. (bottom) Results are mean ± SD of the percent incidence of the phenotype occurring within the total population of transfected cells containing HaloTag signal localized in the cytoplasm or proximal to Golgi from three independent experiments. A single cell may have both HaloTag localizations indicated. Images contained 15-20 untransfected and transfected cells per field. Scale bar = 10 µm. (bottom) Quantification of HaloTag localization in cells transfected with either an empty vector control or UNC-61a $_{1-48.}$ Error bars are mean ± SD of three independent experiments. *, ≤ 0.05, as determined by Multiple Unpaired T-tests. **(E)** (top) Western blots of cytosolic (C) and membrane (M) fractions of HeLa cells transiently expressing either HaloTag empty vector (EV) or UNC-61a $TMD_{1-48}$::HaloTag (UNC-61a $TMD_{1-48}$). Lanes 1-3: whole cell lysate (WCL) blotted singly with antibodies recognizing GM130 (membrane), γ-tubulin (cytosol) and HaloTag. Lanes 4-6 WCL and C and M fractions are probed with a mixture of all three antibodies (GM130, γ-tubulin, and HaloTag). A shorter exposure (4.9 s) was used to image the HaloTag to prevent band saturation. (bottom) Membrane enrichment of HaloTag for the EV and UNC-61a $TMD_{1-48}$::HaloTag was analyzed semi-quantitatively and plotted as the ratio of membrane enrichment to cytosolic enrichment. Plot: mean ± SD of three independent experiments.

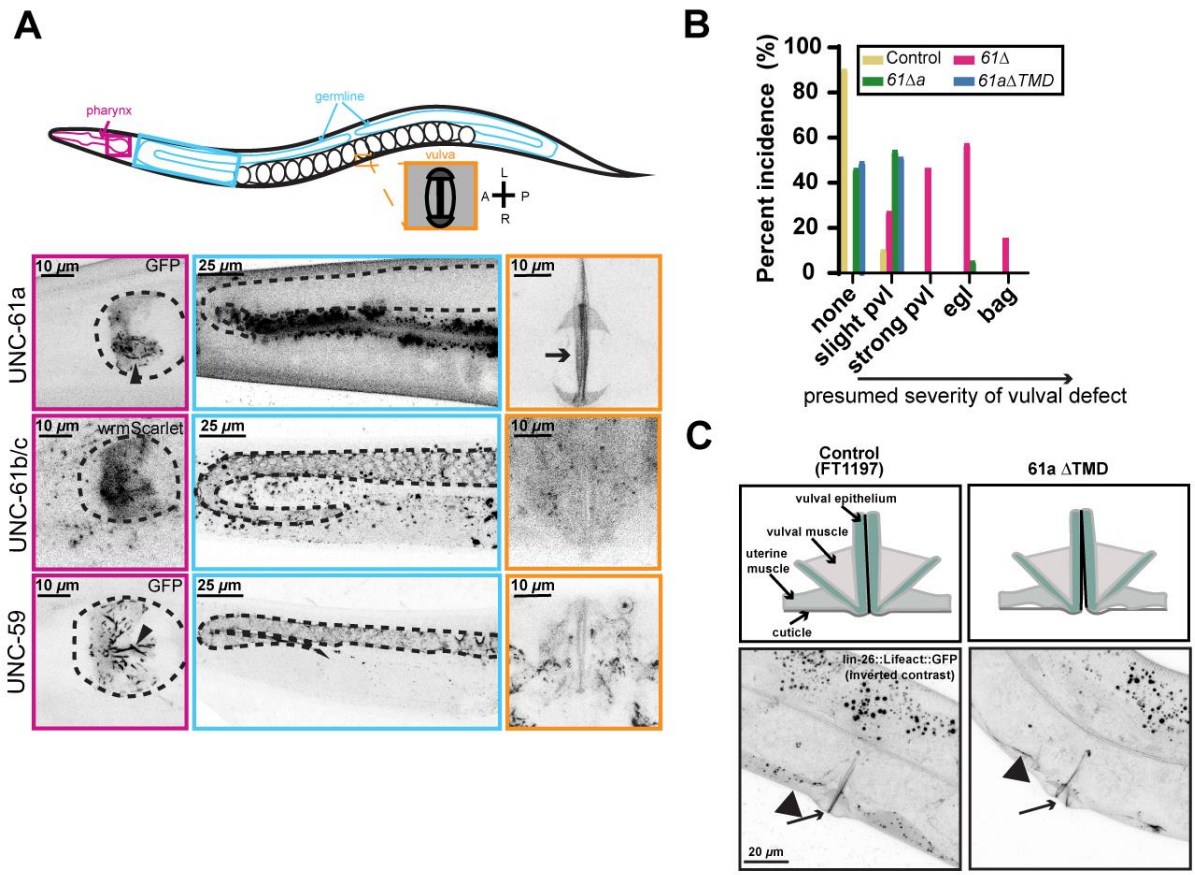


**Fig. 2. UNC-61a TMD is required for normal vulval morphology and function. (A)** (top) Schematic of adult *C. elegans* hermaphrodite (pink: pharynx, blue: germline, orange: vulva.) (bottom) Images are inverted contrast of the fluorophore annotated. Arrow: vulval epithelium apical surfaces; arrowhead; linear septin decorated structures. Dashed lines outline the *C. elegans* terminal bulb and oogenic germline. Scale bar = 10 µm (pharynx and vulva); 25 µm (germline). **(B)** Percent incidence of post-embryonic phenotypes (pvl: protruded vulva; egl: egg-laying defective; bag: bag-of-worms) of control (yellow), 61Δ *(note that you use Δ61 in the panel)* (purple), 61aΔ (green), and 61a ΔTMD (blue) animals (n=100 animals). **(C) (**top) Schematic of control and 61a ΔTMD vulvae (green: epithelium, black: apical surface, grey: surrounding muscles.) (bottom) Inverted contrast images of Lifeact::GFP (F-actin) in vulva region. Arrowhead: muscle cuticle connection in control, disconnection in *unc-61a*ΔTMD; arrows: apical surface of the vulval epithelium. Scale bar = 20 µm.

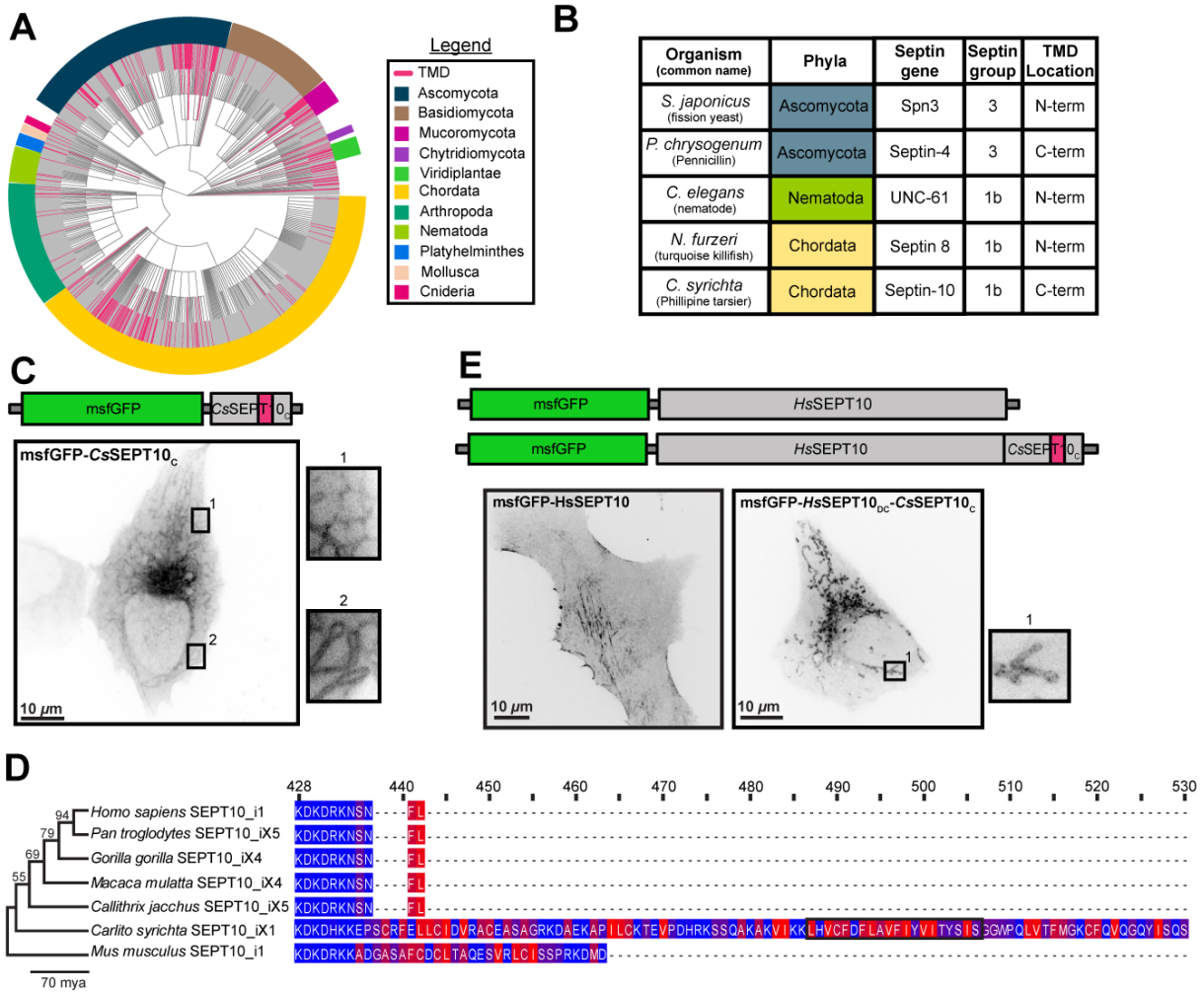


| Organism (common name) | Phyla | Septin gene | Septin group | TMD Location |
|---|---|---|---|---|
| *S. japonicus* (fission yeast) | Ascomycota | Spn3 | 3 | N-term |
| *P. chrysogenum* (Pennicillin) | Ascomycota | Septin-4 | 3 | C-term |
| *C. elegans* (nematode) | Nematoda | UNC-61 | 1b | N-term |
| *N. furzeri* (turquoise killifish) | Chordata | Septin 8 | 1b | N-term |
| *C. syrichta* (Phillipine tarsier) | Chordata | Septin-10 | 1b | C-term |

**Fig. 3. Animal septins are predicted to contain transmembrane domains (TMD).** (A) Cladogram of all septin sequences deposited on UniProt (magenta: sequences containing TMDs). Rim colors: organismal phyla (dark blue: Ascomycota, brown: Basidiomycota, fuscia: Mucoromycota, purple: Chytridiomycota, lime green: Viridiplantae, yellow: Chordata, teal: Arthropoda, light green: Nematoda, blue: Platyhelminthes, light pink: Mollusca, hot pink: Cnideria). **(B)** "Model organisms" with TMD-septins: septin gene, its homology group, and the TMD location. Class color-coded as in (A). **(C)** msfGFP-*Cs*SEPT10$_C$ expressed in U2OS cells. **(D)** Schematic of *Cs*SEPT10 and *Hs*SEPT10 protein architecture. Colors as in Figure 1C. **(E)** Localization of msfGFP-*Hs*SEPT10 and the chimera msfGFP-*Hs*SEPT10$_{\Delta C}$-*Cs*SEPT10$_C$. All images are inverted contrast. Scale bar = 10 µm.